

Single molecule measurements of DNA transport through a nanopore

Amit Meller¹ and Daniel Branton²

(1) The Rowland Institute for Science, Cambridge, MA 02142;

(2) Department of Molecular and Cellular Biology, Harvard University, Cambridge,

MA 02138

Running title: Single molecule measurements of DNA transport through a nanopore

Corresponding author:

Dr. Amit Meller

The Rowland Institute for Science

100 Edwin H. Land Blvd.

Cambridge, MA 02142

Fax: (617) 497-4627

Email: meller@rowland.org

Keywords: translocation, capture, electric field

Summary

We examined the voltage-driven movement of single stranded DNA molecules in a membrane channel or “nanopore.” Using single channel recording methods and a statistical analysis of many single molecule events, we determined how voltage influences capture and translocation in the nanopore. We verified that the mean time between capture events follows a simple exponential distribution, whereas the translocation times follow a unique distribution that is partly Gaussian and partly exponential. Measurements of polymer sequence effects demonstrated that translocation duration is heavily influenced by specific or non-specific purine-channel interactions. The single molecule approach we used revealed molecular interactions that can influence both capture rates and translocation velocities in a manner that enriches naive barrier crossing models.

Introduction

Our understanding of the detailed dynamics and physics of polymer translocation through confining channels across membranes, or through gels, continues to evolve [1,2]. In particular, the relative contributions of polymer-channel interactions and chain entropy are not fully understood. Recently, single-channel ion current measurements have been used to study the translocation dynamics of single-stranded RNA and DNA through atomically characterized channels in an *in vitro* model system [3-6]. In this system a voltage bias drives the charged nucleic acid molecule through a single 1.5 - 2.0 nm pore in a protein channel (α -hemolysin from *S. aureus*) that is incorporated in a phospholipid membrane. The membrane is formed across a micron-sized aperture that separates two ion-containing solutions. Translocation of each nucleic acid polymer is monitored by recording the ionic current modulation or “blockade” that occurs whenever a translocating polymer occupies the nanopore. Although the nanopore detects the presence of only a single molecule at a time, many single molecules can sequentially translocate through the nanopore in a few seconds. Thus, the system provides information about the behavior of single molecules, but because a large number of single molecule events can be recorded in a short period, a statistical analysis is possible. In particular, measuring the blockade level and its associated duration as each molecule translocates through the channel makes it possible to study the fundamental physics underlying the polymer’s motion in the confined space of a nanopore.

The understanding gained from such studies should illuminate our comprehension of more complicated processes, such as the movement of polymers through gels, the complexities of polypeptide transport across a membrane during protein synthesis, or DNA movement during phage injection. From a more practical viewpoint, such measurements can provide information about the base composition of the polynucleotides, its structure and its length. Better quantification of driven translocation may also result in novel ways to discriminate and count DNA molecules [5] and set the stage for a new sequencing method [7].

In this manuscript we examine how the driving force, the electric field in our case, determines the dynamics of DNA translocation. We separate the process into two essential steps. First, the DNA molecules must enter or be captured by the pore. Because the protein channel of our experimental system lacks the architecture that a phage employs to direct its genetic material into the cell, entry into the pore depends on diffusion and the action of the local electric field outside the channel to capture one of the polymer's ends. Second, the molecules are translocated from one side of the membrane to the other side by the electrical potential across the membrane. We characterize the dynamics of capture and translocation at varying electric fields, DNA lengths and base compositions.

Materials and Methods

A single nanopore in a horizontally supported phospholipid bilayer was formed by self-assembly of α -hemolysin from *Staphylococcus aureus* (Calbiochem, CA), as

previously described [5]. The membrane separated two Teflon chambers, each containing ~70 μ l of a buffered saline solution (1M KCl, 10mM Tris, 1mM EDTA, pH 8.5) in contact with Ag-AgCl electrodes. The entire apparatus was embedded in a copper enclosure so that the temperature of all the solutions and components could be regulated to ± 0.05 °C. Proper grounding of the copper block helped reduce electrical noise pick-up. The setup made it possible to maintain a fixed temperature over days, and for some of our experiments a single α -hemolysin pore was used for over 36 hours without a noticeable change in open pore current or stability.

Single stranded DNA samples were purchased from either Midland Certified Reagents (Midland, TX) or from Research Genetics (Huntsville, AL). All polymers below 40 bases were reverse phase HPLC grade and were used without further purifications. The longer polymers (60-100 bases) were size purified in 8% polyacrylamide gels under denaturing conditions. The concentrations of the excised, purified, and eluted molecules were estimated from their 260nm absorption after re-dissolving in 1mM TE buffer at pH 8.5. In a typical experiment, the DNA concentration in the *cis* chamber was brought to about 1 μ M.

With the *cis* side negative, a voltage of 60 – 300 mV was applied across the channel using a patch-clamp amplifier and head-stage (Axopatch 200B and CV203BU, Axon Instruments, Foster City, CA). The ionic current was sampled at 333KHz with a 12-bit analog/digital board (Axon) and the amplified signals were filtered at 100 KHz (3302 filter, Krohn-Hite, Avon, MA). In the 60 – 300 mV range, the measured ionic current through a single, ~1.8 nm pore was linear with the applied voltage (see Figure 1a) and very reproducible. At a constant voltage and over the

2°C-50°C temperature range we used, the temperature dependent ionic current was proportional to the bulk electrical mobility of the potassium-chloride electrolyte (Figure 1b). This result suggests that in the temperature range of interest, our nanopore does not undergo large structural modifications that alter its ionic conductivity.

Figure 2 shows a typical current trace of three translocating DNA molecules. When a molecule enters the pore, the current drops from its initial open pore current (roughly 100pA in this example) to its blocked level (about 10pA). After translocation, when the DNA molecule clears the channel, the open pore current is restored. Between 500 and 7500 translocation events were recorded separately for each type of DNA, temperature and voltage setting. Translocation events, or simply “events”, were defined as those that decreased the current to less than 25% of the open pore value (see Figure 2), and had similar open pore currents before and after translocation. The stored data were analyzed using custom software that calculated the translocation duration, t_D , the normalized blockade current, I_B , averaged over the translocation duration of each event, and the time elapsed between two successive events, δt . Short current spikes whose durations were comparable to, or less than, our ~10µsec electrical response time were rejected by our software, as were events that occurred within periods of variable open pore current levels.

Results

a. Rate and probability of DNA entry

Prior to DNA translocation, a DNA molecule must be transported to the nanopore and one end of the molecule must enter the pore. During entry, the molecules are transported by diffusion that is biased by chemical potentials, external fields, etc. from the bulk to the pore aperture. In some cases molecules that reach the pore on one side of the membrane will not be captured in the pore. These episodes are distinguishable from true entry events because they result in a brief (duration $\ll 10\mu\text{sec}$), partial blockade or downward current spike. Because of finite electronic bandwidth limitations, an unknown fraction of these spikes are actually registered. This fraction was digitally filtered out of our recorded data and only those entries that were followed by a full translocation event were processed. Because only molecules that entered and were subsequently translocated across the membrane are counted in our analysis, henceforth we refer to the entry process as a “capture” event. Full translocations following capture exhibited a clear blockade pattern (see Figure 2) that was characterized by a measurable current level and duration time.

To characterize the entry process and determine whether interactions between polymer molecules should be taken into account, we measured the time gap between successive capture events, δt , at varying conditions such as bulk concentration and applied voltage. For dilute samples where $\delta t \gg t_D$, one can define an average capture rate, $R(C,A,V,T)$ which depends on the bulk polymer concentration, C , the pore cross sectional area, A , the applied electric voltage, V , and the temperature, T [8]:

$$R(C,A,V,T) \propto CA \int f(\vec{v})(\hat{n} \cdot \vec{v}) d^3v, \quad (1)$$

where $f(\vec{v})$ describes the vectorial distribution of molecule velocities in the vicinity of the pore that may depend on the external electric field, \vec{v} is the center of mass velocity, and \hat{n} is a unit vector perpendicular to the pore aperture. The proportionality sign reflects the fact that only a fraction* of the molecules that collide with the pore will do so in a manner that favors capture of one or the other end of the molecule in the pore. In the absence of external fields, $f(\vec{v})$ should be reduced to the Maxwellian distribution. It is important to note that this formulation depends strongly on the assumption that the system is dilute and that polymer-polymer interactions can be neglected. We do not know *a priori* that this is indeed the case in our experiment since the polymer concentration adjacent to the pore might be significantly higher than in the bulk.

To determine if polymer-polymer interaction can be neglected, we assume that the rate, R , is stationary and define the probability of observing zero capture events, P_0 , at time t (t is measured from the occurrence of the last event). For a given average event rate, R , $P_0 = (1 - R\Delta t)^{t/\Delta t}$ where Δt is an arbitrary small time slot. Then taking the limit $\Delta t \rightarrow 0$ we get:

$$P_0(Rt) = e^{-R(C,A,V,T)t} \quad (2)$$

To check this simple prediction we measured the distribution of times between successive events, δt , for three different polymer types at different concentrations and calculated the corresponding distributions (Figure 3). All the polymers we tested

* In the absence of an external field, the number of molecules expected to collide with the pore is ~200 per second for our experimental conditions [9] (40mer DNA, at 1 μ M in bulk). This value is about 4 orders of magnitude larger than the number of entries (~0.01sec⁻¹) measured at a voltage just marginally above the minimal voltage that supports translocation.

showed a remarkably clean exponential behavior over more than two decades. The average capture rates were readily extracted from the exponential fits to the three experiments and were found to be $13.05 \pm 0.55 \text{ sec}^{-1}$ for poly(dA)₂₀, $10.45 \pm 0.52 \text{ sec}^{-1}$ for poly(dCdCdTdCdC)₆, and $2.93 \pm 0.14 \text{ sec}^{-1}$ for poly(dC)₄₀. Normalizing these values by the corresponding DNA molar concentrations of the three samples (2.3, 1.8 and 0.5 μM) we found a single value, $5.8 \pm 0.1 (\text{sec } \mu\text{M})^{-1}$. This normalized capture rate was weakly dependent on the type of DNA, but strongly dependent on the electrical potential and the temperature. We note that this method yields a better measure of the error in R than simply counting the number of events per minute because it makes use of the exponential distribution. The same raw data sets were used to extract the probability distribution, P_n , for $n = 0, 1, 2, 3 \dots$ events, for a given polymer rate, and time window size, dt . To compare the three data sets, we adjusted dt in each case to account for the different DNA concentrations such that for each case $R \cdot dt = \text{const}$. These distributions overlapped and formed a single Poissonian curve (Figure 3, inset), with:

$$P_n(R \cdot dt) = \frac{e^{-Rdt} (Rdt)^n}{n!}.$$

The line in this figure is a single parameter fit to the three data sets. We repeated the experiment with other polymer types under variable conditions (applied voltage, temperature and concentration) and essentially all our data reproduced the same curve. The fact that bulk concentration normalized all of the measured capture rates, R , to a single value indicates that this rate is indeed proportional to the *bulk concentration* (at 120mV). This result supports our assumption that the system can

be regarded as a dilute system in which interactions between polymers can be neglected. Deviations from this behavior were observed at high electrical fields (e.g. over 140mV) as discussed below, or when the bulk concentration was significantly increased.

In the most simplified description of the process, a successful capture event could be seen as crossing a barrier, U' , that can be surmounted because of an electrical potential ΔU . The value of ΔU can be calculated from $\Delta U = nze\delta V$, where n is the number of monomer units (phosphates) in the electric field, ze is the effective monomer charge, and δV is the electric field drop over the energy barrier for the end of the molecule to enter and be captured by the pore. In this picture the capture rate will follow a simple Van't Hoff-Arrhenius relation intensity [10,11] $R \propto \exp(-(U' - \Delta U)/k_B T)$. Here we make the distinction between δV and the total electric field, V , measured at the electrodes. The proportionality constant in the last expression is related to the *local* concentration of molecules near the pore, and the polymer probability to be captured. At relatively low potentials we expect that the local concentration of molecules near the pore will approximate the bulk concentration. But at higher potentials, the local DNA concentration could be skewed by the potential field. Our results (see below) suggest that the cross-over between the two regimes occur between 120-140mV.

By using low temperatures we were able to extend the measurement of capture rate to voltages as high as 250 mV without losing the ability to distinguish between true entries and current spikes (Figure 4). The capture rates could be approximated by a sum of two exponents (two straight lines on this plot) separated by

a cross-over region (120 – 140mV). In each of the two regions, the slopes of the data sets were similar for the two bulk concentrations tested but, as expected, the ratio of the amplitudes of the exponentials were close to the bulk concentration ratios ($2.6/0.9 = 2.9$).

In the low voltage region we can extract the exponents (the slope on the semi-log plot) for the two polymer concentrations. These values could be used to obtain an estimate for $nz \approx 1.9$ since the slope, $0.075mV^{-1} = nze/k_B T$, and $k_B T/e \approx 24mV$ ($T = 5^\circ C$). This value for $nz \approx 1.9$ is in a good agreement with the one reported for the 60 –120mV voltage range[10]. But we note that this value probably does not represent the full effective charge on the DNA because the actual potential drop that induces the end of the polymer to enter the pore would be significantly smaller than V , the electrode to electrode field measured in our experiment. With the 1M ionic strength solution used in these experiments, δV is expected to be much smaller than V . Hence, the ≈ 1.9 value calculated above for nz underestimates its real value. To derive the correct value of δV on the cis side of the nanopore, one should take into account access resistance effects [12] and carry out a detailed solution of the electromagnetic-hydrodynamic velocity field distribution in the vicinity of the pore. This calculation is beyond the scope of the current paper.

Above $\sim 140mV$ the rate dependence on V is much weaker than in the <120 mV regime. The ratio of the exponents ($exp <120 \text{ mV}/exp >140 \text{ mV} \approx 5$) in the two regimes can be accounted for in two ways. First, at low voltages we estimate the ratio of collisions to captures to be roughly 10^4 to 1. If this ratio is roughly maintained at the higher capture rates seen above 140 mV (Figure 4), then the

number of collisions could easily exceed $\sim 10^5 \text{ sec}^{-1}$ when the voltage bias exceeds 140 mV. As a consequence, polymer-polymer interactions, i.e. collisions and intermolecule repulsion will limit the probability of polymer ends entering the pore. Second, we note that while the number of capture events per unit time exhibits an exponential increase with voltage, the most probable translocation time, t_p has a weaker $\sim V^{-2}$ dependence [6]. Therefore at sufficiently high voltages the assumption that $\delta t \gg t_D$ is not valid, and capture rate may be limited by the time taken for the polymers to translocate through the pore. To illustrate this point, if one were to extrapolate the initial exponential dependence of capture rate on voltage shown in Figure 4 to 200mV, one would predict a capture rate of $\sim 2,000 \text{ sec}^{-1}$. This value corresponds to an average elapsed time between events of $\overline{\delta t} \approx 0.5 \text{ msec}$. At the same time the t_p values for this polymer at 200mV would be in the range between 0.05 – 0.5 msec (unpublished data). Therefore the assumption that $\delta t \gg t_D$ is no longer valid, and we would expect a noticeable deviation from the original exponential slope. It is also interesting to notice that during translocation, most of the ionic current ($\sim 90\%$) is blocked. Thus the electric field distribution near the pore is abruptly, but temporarily, modified. When the event rate is relatively low these perturbations can be neglected. At high event rates they become very significant. Although our arguments explain why there must be a deviation from the initial exponential dependence at higher voltages, it does not account for the observation that the cross-over at different concentrations occurs at roughly the same voltage range (120 – 140 mV, figure 4). We believe that a self-consistent electrodynamic

solution of the electric field distribution in the vicinity of the pore may account for this observation.

b. DNA translocation

During translocation, the polymer is partitioned between the two compartments (assuming that it is long enough), with n monomer units on the *trans* side and $N - n - d/a$ units not on the *trans* side, where N is the total number of monomer units in the polymer, d is the length of the channel, and a is the length per unit monomer such that d/a is the number of monomer units inside the channel. Crossing from one side to the other side involves hopping over a free energy barrier that includes both entropic [13,14] and enthalpic terms, including depletion of water and ions from the channel by the polymer [1], and specific and non-specific interactions between the DNA and the protein residues lining the nanopore. All these contributions are balanced against the electric driving force to produce the DNA motion and should be taken into consideration when describing the polymer dynamics.

The translocation dynamics of each molecule were characterized by two quantities: the average blockade current, I_B , and the translocation duration time, t_D . Our prior work [5] showed that although the blockade current distributions are well fitted by a Gaussian curve* (Figure 5), the translocation time distributions were

* The normal Gaussian distribution of the blockade current reflects the fact that I_B is an average of the current values measured during the entire time of a translocation event and that each current value measurement is, in any case, the consequence of the ~ 12 bases that span the channel [6].

always characterized by a sharp rise followed by a nearly-exponential tail function (Figure 6). Thus, the most probable value, t_p , was much shorter than the *mean* translocation time.

To characterize the specificity of polypurines' or polypyrimidines' interaction with the pore, we compared the translocation time distributions for homopolymers of poly(dA) and poly(dC). The polydeoxycytosines translocated almost 3 times faster than did the polydeoxyadenines (Figure 6). It could be hypothesized that the slow translocation of poly(dA) is in part attributable to the strong tendency of poly(dA) to exhibit base stacking that would make the polymer more rigid. To test this hypothesis, we constructed single stranded DNA polymers with varying numbers of adenines evenly spaced in cytosine polymers. The association constant for dA-dC stacking is less than half that for dA-dA stacking [15]. If base-stacking interactions were a predominant factor that limited the rate of DNA translocation, and thus increased t_p , we would expect that polymers with a contiguous sequence of adenines would translocate more slowly than polymers with adenines interspersed within cytosines. In fact, our results were quite the opposite: a few evenly spaced single adenines in a predominantly cytosine polymer markedly slowed polymer translocation, whereas increasing the number of adenines beyond 50%, where one adenine could stack with a contiguous adenine, caused only a mild decrease in the polymer's translocation rate (Figure 7). These results can be interpreted as the result of either specific interactions between adenines and a finite number of sites lining the nanopore wall, or as the result of non-specific friction-like interactions as the large adenines are driven through the narrow confines of the nanopore. Control molecules,

such as pure poly(dC) into which increasing numbers of evenly spaced (dT)s were incorporated, exhibited strictly linear changes in t_p (Figure 7). These linear changes in t_p with increasing numbers of (dT)s in poly(dC) would be expected if each (dT) monomer unit contributed its characteristic t_p in a simple additive manner, without extraneous effects due to interactions with the nanopore wall.

The relative importance of adenine-nanopore wall interactions vs. adenine stacking interactions was emphasized by comparing t_p for poly(dCdA)₅₀ and polydA₅₀dC₅₀ polymers. Each of these two polymers has the same number of dAs and dCs, but dA-dA base stacking cannot occur in poly(dAdC)₅₀. Therefore, if base stacking significantly increase t_D , one would expect poly(dAdC)₅₀ would translocate much faster than polydA₅₀dC₅₀. In fact, poly(dAdC)₅₀ translocation was slower than poly(dAdC)₅₀ (Figure 8). Furthermore, the difference between t_p of the pure adenines and t_p of the pure cytosines increased at lower temperatures. This suggests that the interactions of the adenines with the pore were stronger at lower temperatures. The relatively steep and non-exponential temperature dependence (best approximated by a $\sim T^{-2}$ dependence) implies that a simple Arrhenius description does not account for polymer dynamics.

Probing the interactions between the channel and the DNA is most efficiently investigated by using short pieces of DNA whose length approximates that of the channel. With such short polymers, the entropic contributions associated with the leading and trailing ends of the polymer outside of the channel do not have to be considered. Our discovery that DNA transport can be significantly slowed at low

temperatures [5] made it possible to study very short polymers without significant detection resolution loss.

We measured the translocation time distributions for varying polymer lengths, N , in the range 4 to 100. Since the interactions between the channel and the polymer take place inside the channel we expected that a marked transition would be noticed when the polymer length exceeded that of the channel. In Figure 9 we depict t_p obtained in the same way that was described earlier as a function of the polymer length, measured in monomer units, for poly(dA) (solid circles) and alternating dCdT (squares) polymers. In both cases, for $N > 12$ we observed a linear regime, where $t_p \propto N$. But for shorter polymers, the dependence on N became steeper, indicating that polymer-pore wall interactions play a major role in determining the rate of translocation. The transition was sharper (indicated by a steeper slope in the curves) for poly(dA) than for poly(dCdT), as would be expected if the interaction between adenine and the pore wall were stronger than that between either cytosine or thymidine and the pore wall. Note that the transition point (at 12 bases) corresponds to a length of 12 bases \times ~ 0.5 nm/base \cong 6 nm; very close to the length of the channel stem that is embedded in the membrane.

To better understand this transition, we calculated the average velocity of the molecules under the simplifying assumption that the rate of translocation was uniform (Figure 9, inset). Above the transition length ($N > 12$) the long polymers translocated at a constant velocity of 0.015 nm/ μ sec. But below the transition length, the polymers clearly translocate faster: removing 2-3 bases resulted in an increase of roughly a factor of 2 in the translocation velocity. This steep dependence on length

supports a picture in which multiple contacts along the channel are responsible for the strong interactions between the DNA and the protein, and these interactions play a significant role in determining the translocation dynamics, particularly for short molecules.

The electrical force acting on the DNA is proportional to the number of unit charges residing inside this channel portion (assuming that the field gradient outside the channel is very small compared with the voltage gradient inside the pore). Long polymers ($N \gg 12$) will experience a constant force since they will almost always experience the field gradient along the full length of the nanopore. For long polymers with repeating base sequences, the polymer-protein interactions are also constant. Thus the translocation times will be simply proportional to the total length of the polymer. But for short polymers ($N < 12$) that do not extend the full length of the channel, a different balance between the driving electrical force and the polymer-pore wall interactions is attained for each polymer length. The consequence is that the rate of translocation shows a steep dependence on polymer length.

Concluding remarks

Our measurements made it possible to analyze the distribution in time of both capture and translocation events. For capture, we find that δt follows a simple exponential distribution (see Figure 3). Thus, the mean time between events is equal to simply the inverse of the capture rate. On the other hand, for translocation, we find that t_D follows a unique distribution that is partly Gaussian and partly exponential

(see Figure 6). Thus, the most probable translocation time, t_p , is much shorter than the average of the translocation times. Together, these results emphasize the additional information contained in analyses that take into account the *distribution* of data points, which can only be obtained by single molecule analysis.

We made use of the observation that poly(dA) translocates through the pore more slowly than does poly(dC) to determine how t_p scales with the number of adenines in the polymer. We also determined how t_p scales with polymer length for polymers shorter than the channel length. Both of these determinations lead us to conclude that translocation duration is heavily influenced by specific or non-specific polymer-channel interactions [16], possibly at multiple sites along the length of the channel. Because of this multiplicity of interaction sites, and because the monomers of a DNA polymer are covalently connected, the rate of translocation depends on more than the specific purine or pyrimidine nucleotide content. It is also sensitive to the nucleotide sequence.

In our system, both capture and translocation events are driven by the voltage bias applied across the membrane. We found that while the capture rate follows an exponential dependence on V , the rate of translocation scales as V^2 . We therefore expect that for some specific parameter range values (e.g., $T = 15^\circ\text{C}$, $C = 2.6\mu\text{M}$, $V \cong 200\text{mV}$) these processes will be coupled, because the two time-scales overlap, and the capture of a new molecule cannot occur while the pore is processing another one. This may explain the deviation that we see from the single exponential of the capture rate dependence when $V > 140\text{mV}$. Moreover, because the membrane is thin, the bias across the channel tends to be large, but a portion of the field also interacts

with the molecule outside the pore. It will be important to understand the microscopic properties of these gradients because they produce molecular interactions that can influence both capture rates and translocation velocities in a manner that enriches naive barrier crossing models.

Acknowledgments

We would like to acknowledge L. Nivon and S. Henrickson for their dedicated help in performing experiments leading to Figures 7 and 9. We also acknowledge C. Sabanayagam and E. Brandin for their help in sample preparations. A.M. would like to thank C.R. Cantor, M. Burns and T. Tlusty for stimulating conversations. Research supported by US Defense Advanced Research Projects Agency, and by the Rowland Institute for Science.

Figure captions

1. Ionic current through a single α -hemolysin pore. (a) The current as a function of voltage (measured at 2°C in 1M KCl buffer) yields a linear dependence with zero intercept. (b) Data points show the current as a function of sample for $V = 120\text{mV}$, measured in the range 2 – 50 °C. The line represents the bulk mobility of 1M KCL ions in arbitrary units. Because the data was obtained from several different channels, the close match between the curve and our data points reflects the reproducibility of the protein channel and its stability.
2. Translocation events. When the DNA polymers enter the pore, the current drops from its initial value of $\sim 100\text{pA}$ to a blocked current of $\sim 10\text{pA}$ ($V = 120\text{mV}$). This blocked current value is observed during translocation of the polymer through the pore and the current is restored to its original value when the DNA exits from the other side of the membrane. Three successive translocation events are displayed. We denote the duration time of each event as t_D , and the elapsed time between events as δt . The average blocked current value, I_B , was also measured.
3. Normalized distributions of the elapsed time between successive capture events. Three polymer types and concentrations are plotted: squares, $(\text{dA})_{20}$ at $2.3\mu\text{M}$; triangles, $(\text{dCdCdTdCdC})_6$ at $1.8\mu\text{M}$; circles $(\text{dC})_{40}$ at $0.5\mu\text{M}$. The elapsed time distributions were obtained by measuring δt for more than 5000 events for each polymer type. In each case, the distributions were normalized to the total number of events. For a large number of events, these distributions are

proportional to the probability of having zero events in a time interval δt , denoted $P_0(\delta t)$. The solid lines are exponential fits (see text) that can be used to extract the event rate and its error. Inset: The same raw data was used to calculate the probability to observe $n = 0, 1, 2, \dots$ events in a time interval dt after adjusting $R \cdot dt$ to be constant for the three samples.

4. Semi-log plot of capture event rate as a function of applied voltage, V . Events were measured as described in Figure 3 using for poly(dC)₄₀ at two different concentrations: circles, 2.6 μ M; squares, 0.9 μ M. The data exhibit two regimes that are well approximated by two exponential fits with a transition between the regimes at ~ 120 -140mV. Above the transition, our assumption that the polymers do not interact with themselves is probably not valid (see text).
5. Distribution of the average blockade current for ~ 1000 translocation events of poly(dA)₂₀. The average blockade current is expressed as I_B , which is the average blocked current value during translocation divided by the average open pore current value over 150 μ sec just prior to each event. A Gaussian distribution (solid line) approximates the data very well.
6. Translocation duration time distributions. A histogram of the t_D values measured for poly(dC)₁₀₀ (left curve), and poly(dA)₁₀₀ (right curve) at 20°C. The shapes of the distributions are typical: for times less than the peak value, the curve follows a relatively steep rise, but for times greater than the peak value it is well approximated by an exponential decay. Because of this non-Gaussian distribution the most probable translocation time, t_p (the peaks), are much

shorter than the mean translocation time $\overline{t_D}$. The t_p values for the poly(dC) and poly(dA) are 120 and 330 μsec , respectively.

7. The effect of purines or pyrimidines on translocation times. The most probable translocation time, t_p , was extracted, as in Figure 6, for a set of 100mers with evenly spaced dA's or dT's in poly(dC) polymers. Because the minority population of deoxynucleotides was evenly spaced in the polymer, when fewer than half of the deoxynucleotides are adenine or thymine, no self-stacking of adenine or thymines can occur. The fraction of adenines (solid triangles, $T = 17.5^\circ\text{C}$) or thymines (open circles, $T = 18^\circ\text{C}$) is denoted as percentages. The large error bar on the 100% poly(dT) data point reflects the fact that it was extrapolated from higher temperature measurements on the same molecule.
8. Translocation duration times for different polymers (reproduced from [5]). The most probable translocation time, t_p , plotted as a function of temperature for poly(dA)₁₀₀ (inverted triangles), poly(dC)₁₀₀ (squares), and two mixed polymer of identical composition but different sequence, poly(dAdC)₅₀ (upright triangles) and poly(dA)₅₀(dC)₅₀ (circles). As expected, the most probable translocation times for the di-block poly(dA)₅₀(dC)₅₀ matches closely the average t_p s (dashed line) of pure poly(dA) plus pure poly(dC).
9. The dependence of t_p on polymer length, N . The most probable translocation duration time, t_p , was measured for poly(dA) (circles) and poly(dCdT) (squares) at 2°C . For $N > 12$ the translocation time is proportional to the polymer length. Shorter polymers exhibit a sharp transition below $N = 12$. Inset, the average

polymer velocity, calculated from t_p values and polymer trajectories during translocation [6].

References

- [1] Bezrukov, S. M. *J. Membr. Biol.* 2000, *174*(1), 1-13.
- [2] Cantor, C. R., Smith, C. L., *Genomics : the science and technology behind the human genome*, John Wiley & Sons, Inc., New-York, 1999.
- [3] Kasianowicz, J., Brandin, E., Branton, D., Deamer, D. *Proc. Natl. Acad. Sci. U.S.A.* 1996, *93*, 13770-3.
- [4] Akeson, M., Branton, D., Kasianowicz, J., Brandin, E., Deamer, D. *Biophys. J.* 1999, *77*, 3227-33.
- [5] Meller, A., Nivon, L., Brandin, E., Golovchenko, J., Branton, D. *Proc. Natl. Acad. Sci. U.S.A.* 2000, *97*, 1079-1084.
- [6] Meller, A., Nivon, L., Branton, D. *Phys. Rev. Lett.* 2001, *86*, 3435-38.
- [7] Andersen, O. S. *Biophys. J. (New and Notable)* 1999, *77*, 2899-2901.
- [8] Huang, K. *Statistical Mechanics*, 2nd ed., John Wiley & Sons, New-York, 1987.
- [9] Berg, H. C., Purcell, E. M. *Biophys. J.* 1977, *20*, 193.
- [10] Henrickson, S. E., Misakian, M., Robertson, B., Kasianowicz, J. *J. Phys. Rev. Lett.* 2000, *85*, 3057-60.
- [11] Haenggi, P., Talkner, P., Borkovec, M. *Rev. Mod. Phys.* 1990, *62*, 251-341.
- [12] Hille, B. *Ionic Channels of Excitable Membranes*, 2nd ed., Sinauer Assoc. Inc., Sunderland, MA, 2001.
- [13] Muthukumar, M. *J. Chem. Phys* 1999, *111*, 10371-74.
- [14] Chuang, J., Kantor, Y., Kardar, M. *preprint cond-mat/0108275* 2001.
- [15] Solie, T. N., Schellman, J. A. *J. Mol. Biol.* 1968, *33*, 61-67.

- [16] Lubensky, D. K., Nelson, D. R. *Biophys. J.* 1999, 77, 1824-38.

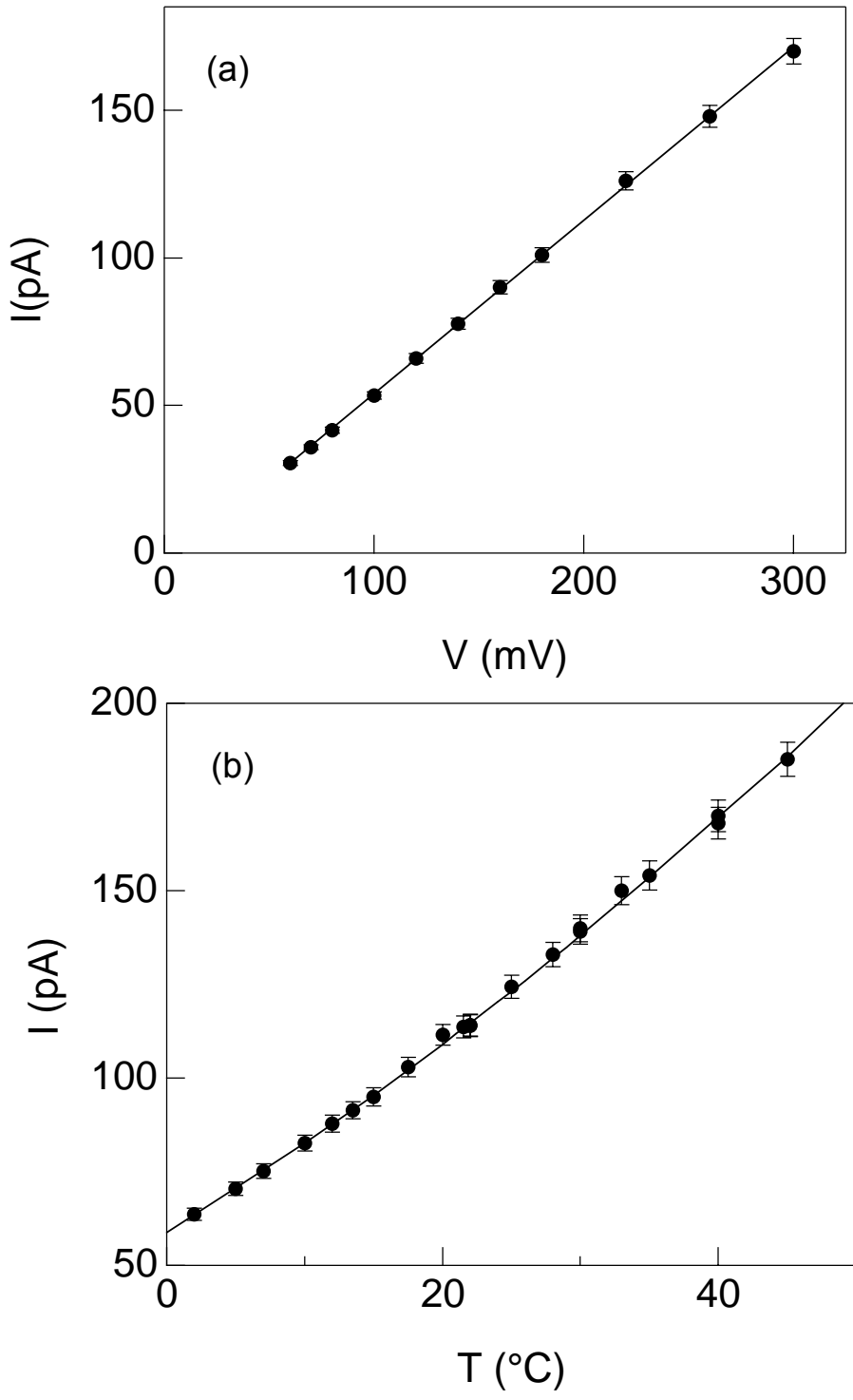


Figure 1

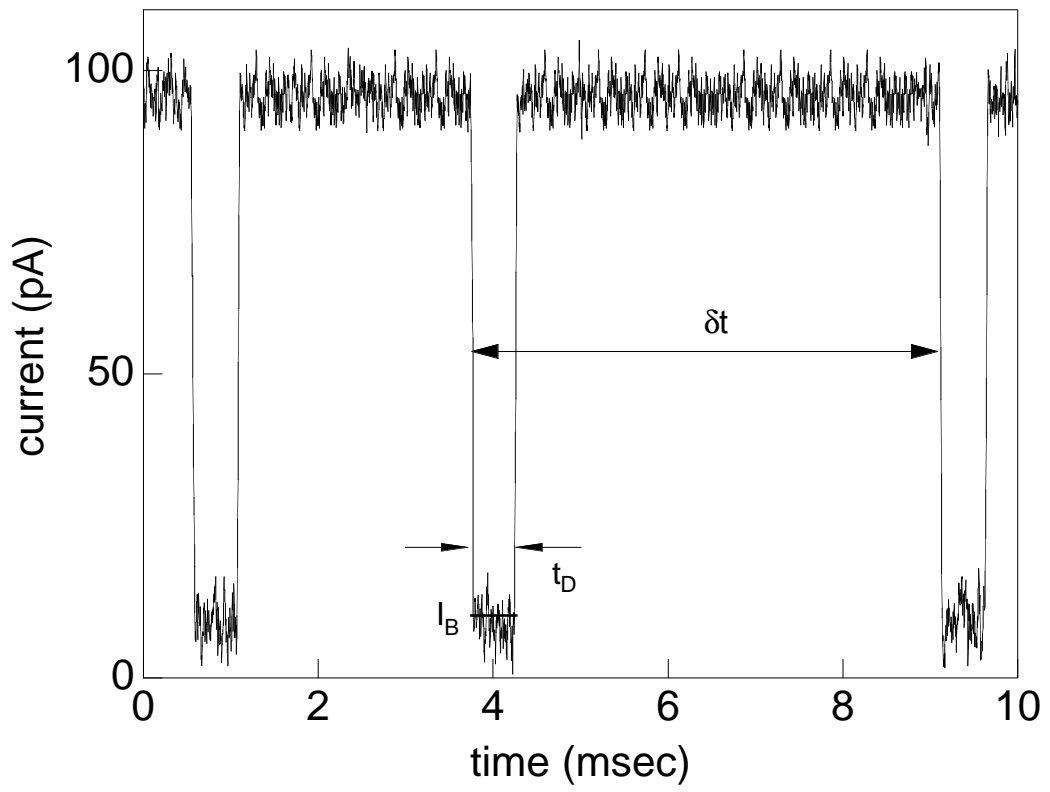


Figure 2

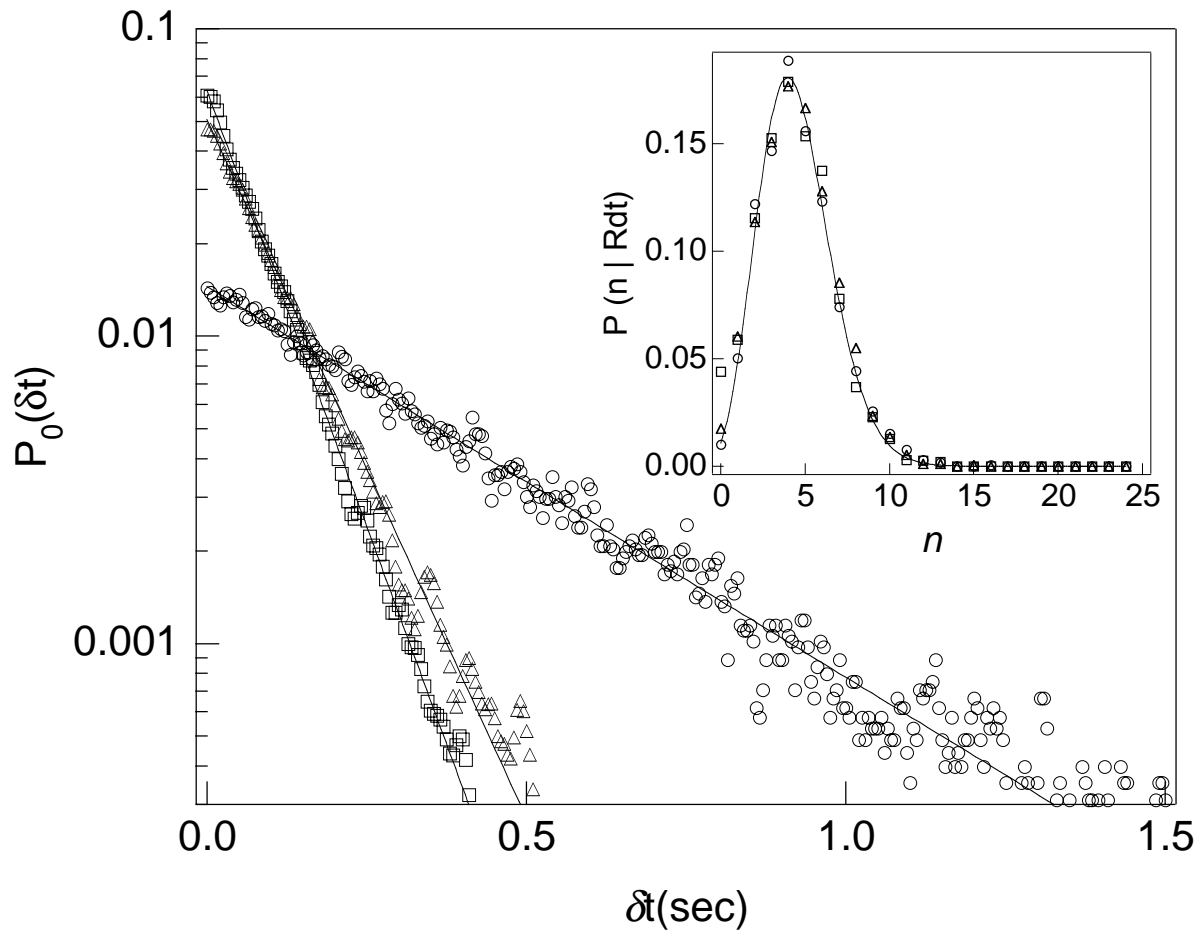


Figure 3

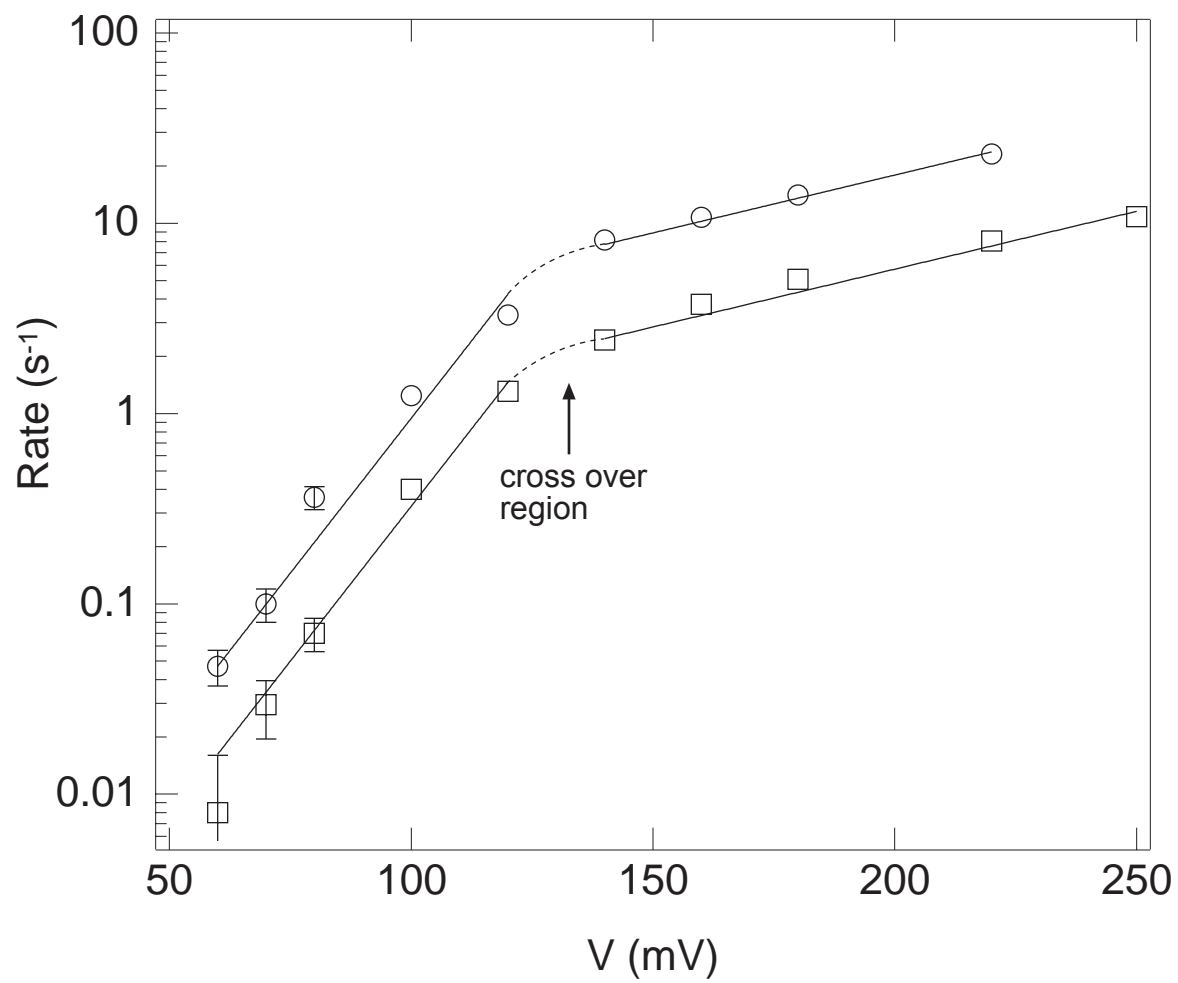


Figure 4

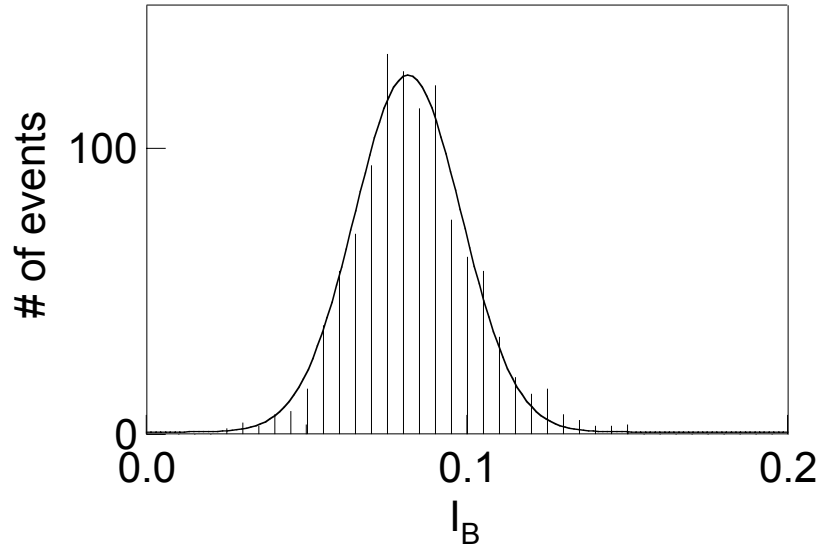


Figure 5

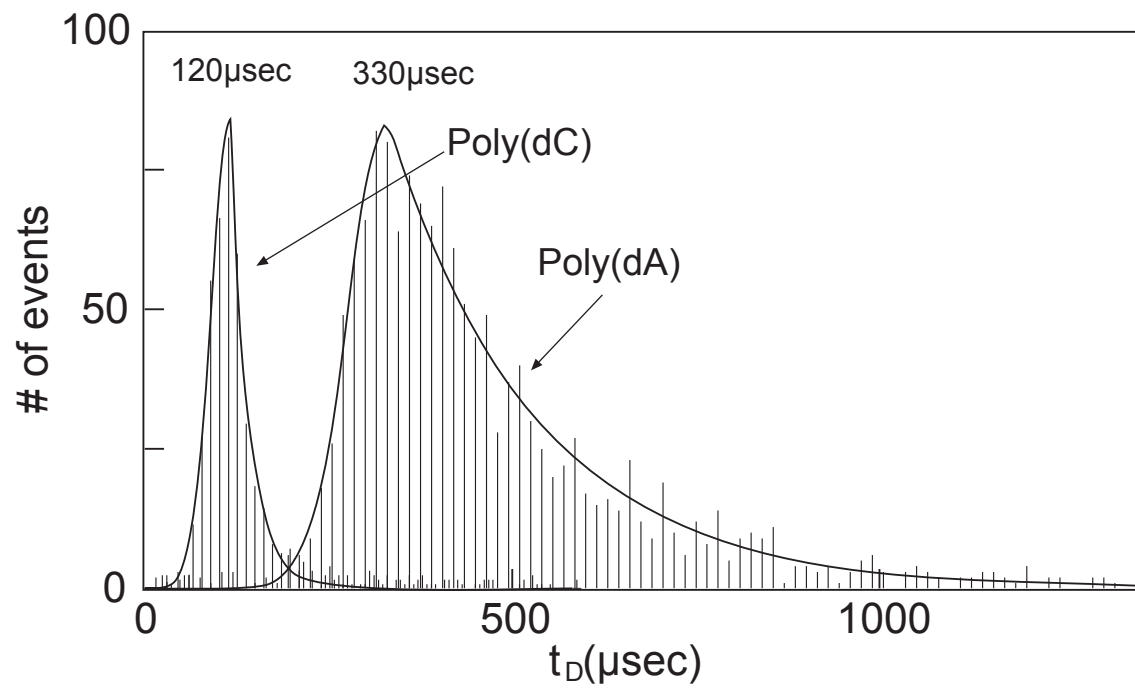
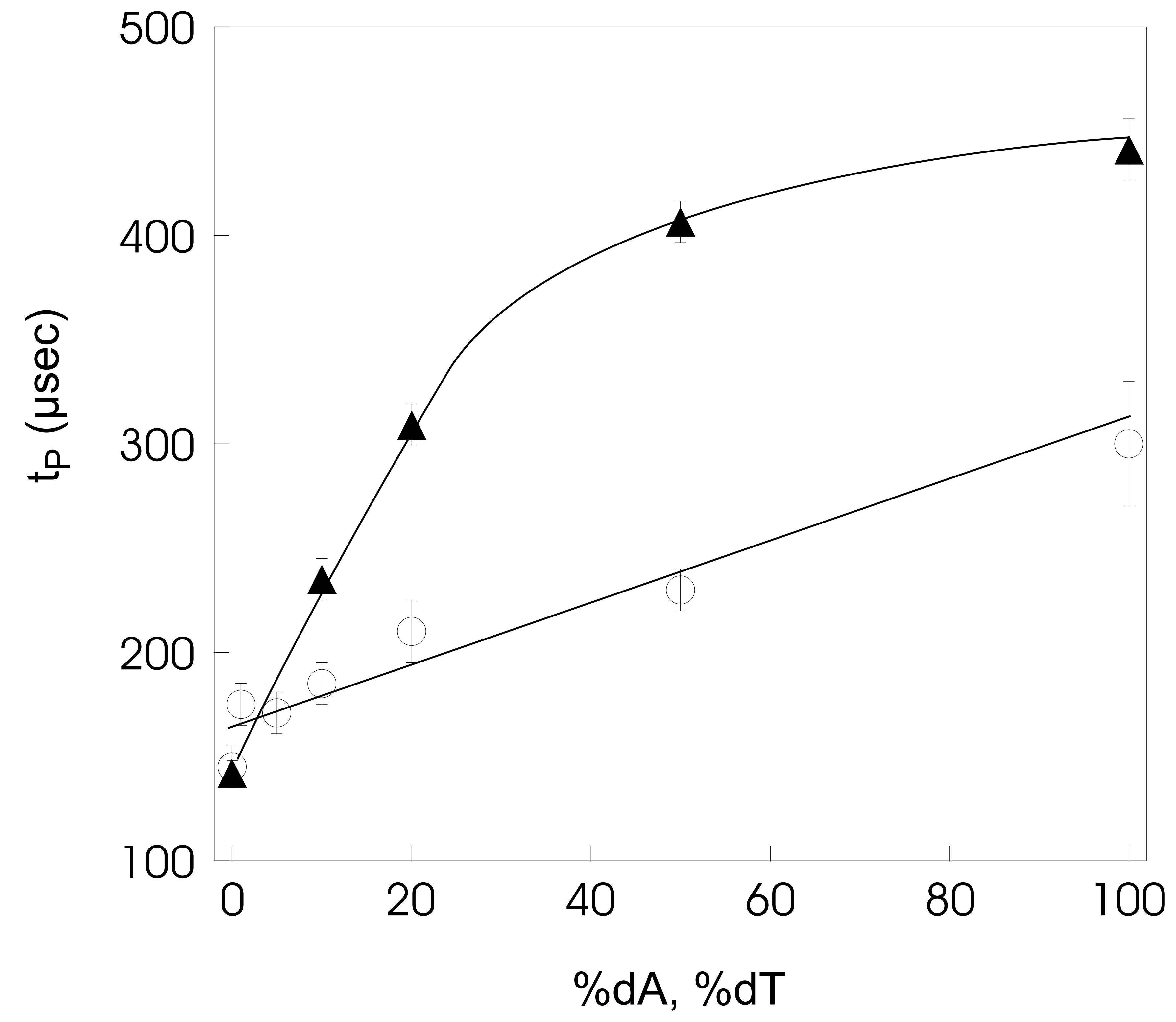


Figure 6



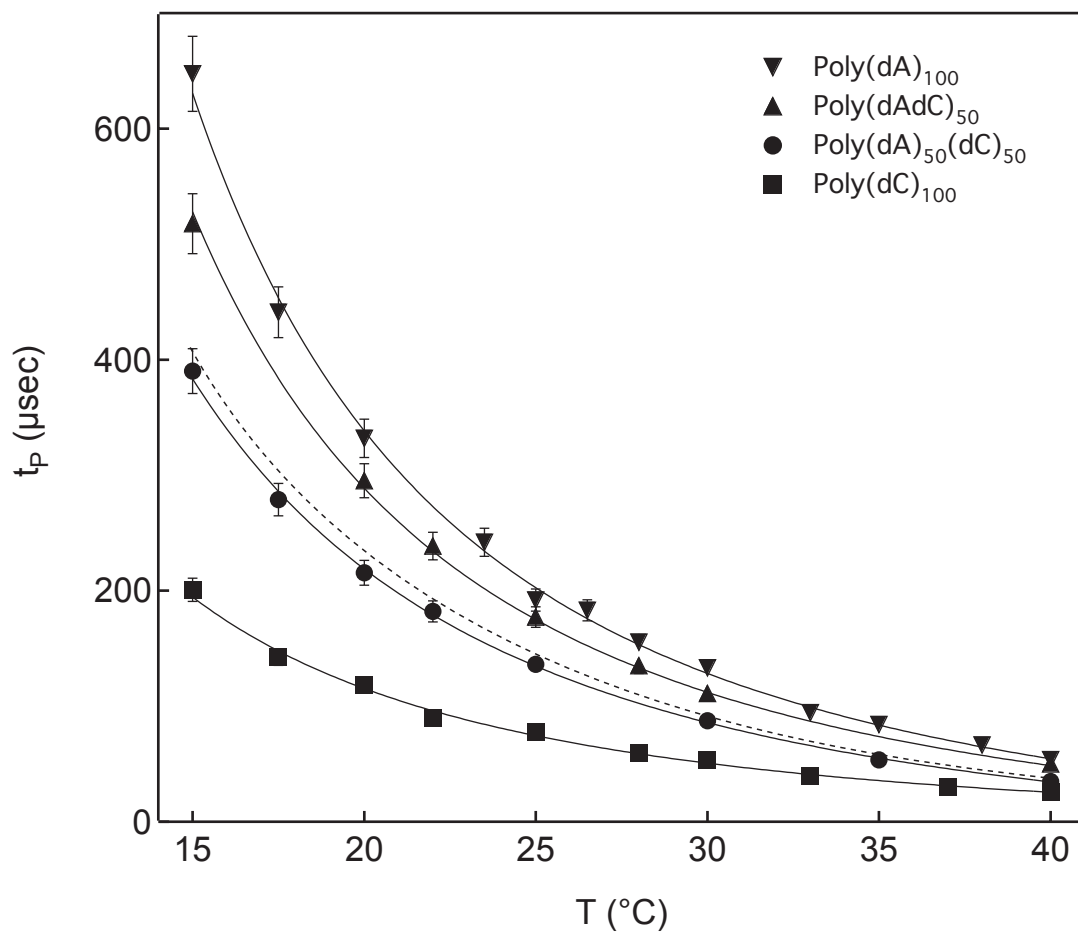


Figure 8

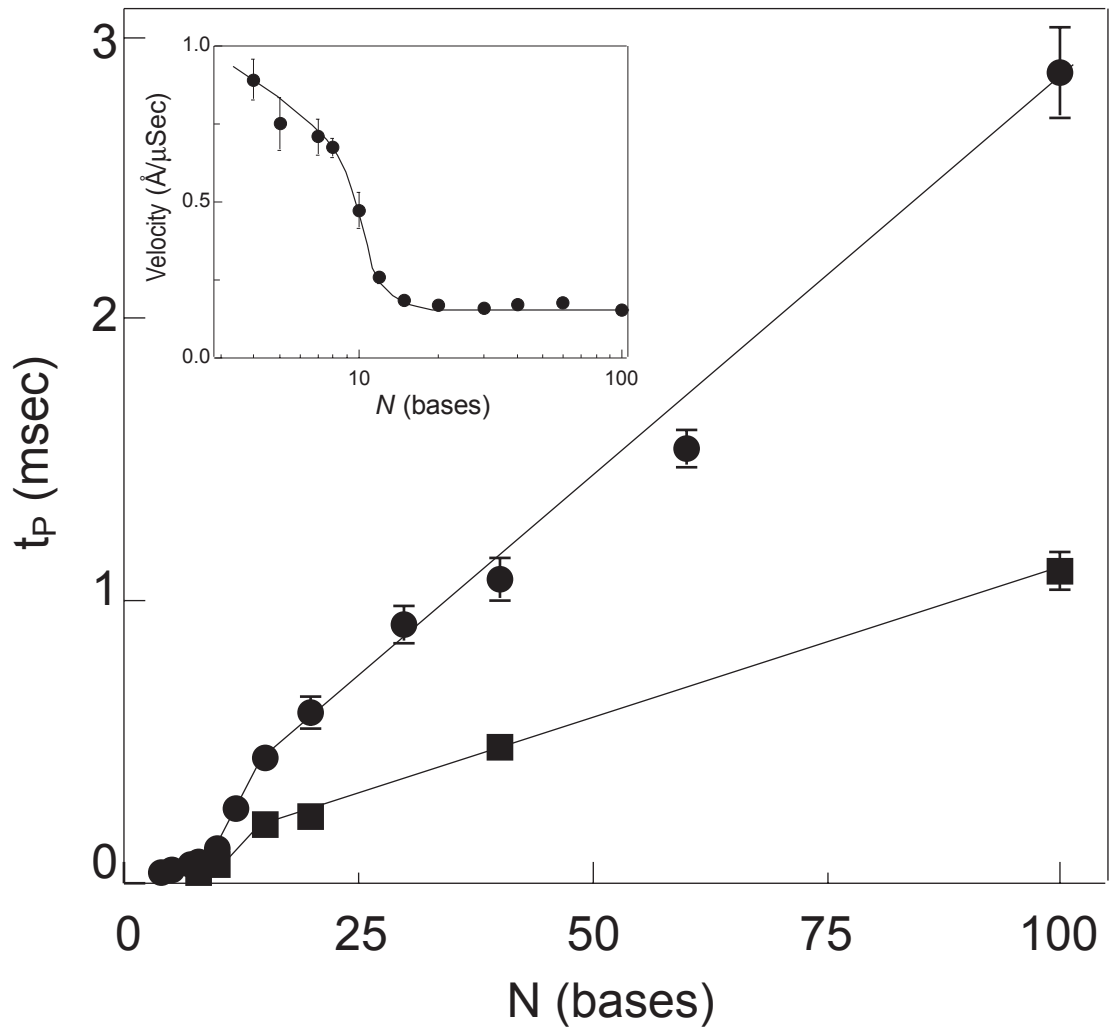


Figure 9